



ACOUSTIC SCATTERING BY TWO SPHERES: MULTIPLE SCATTERING AND SYMMETRY CONSIDERATIONS

P. GABRIELLI AND M. MERCIER-FINIDORI

URA 2053 CNRS, Systèmes Physiques pour l'Environnement, Equipe Ondes et Acoustique,
Université de Corse, Faculté des Sciences, 20250 Corte, France

(Received 25 November 1999, and in final form 8 August 2000)

Acoustic scattering by two identical spheres is theoretically, numerically and experimentally studied by highlighting the role of the symmetries of the scatterer. Incident and scattered fields are expanded over the different irreducible representations of $D_{\infty h}$, the continuous symmetry group of the scatterer. Then, from the boundary conditions, one obtains for each irreducible representation an infinite system of linear complex algebraic equations where the unknown scattering coefficients are uncoupled. This feature greatly simplifies the treatment of the problem and speeds up calculations. Farfield form functions are computed in the cases of Neumann boundary conditions (rigid spheres) and elastic boundary conditions (elastic spheres immersed in water). A series of experiments based on ultrasonic spectroscopy is performed in the case of two stainless-steel spheres immersed in water. The comparison between the theoretical and the experimental results provides quite a good agreement.

© 2001 Academic Press

1. INTRODUCTION

Acoustic scattering by many bodies of various shapes has been the subject of several works during the last 40 years. A general and widely spread way to treat scattering problems by many objects that are relatively close to each other is by using the techniques of multiple scattering [1, 2]. The multiple-scattering formalism can be simplified by taking into account the symmetry properties of the scatterer. Symmetry considerations are extensively used in quantum physics with, for instance, applications in crystallography [3], in electromagnetism [4] and in quantum chaos [5, 6]. Recently, symmetry properties have been used for the first time in acoustics. In order to simplify the multiple-scattering formalism the two-dimensional problem of acoustic scattering by two identical cylinders has been studied, highlighting the role of the symmetries of the system [7]. In this work, incident and scattered fields are expanded over the different irreducible representations of \mathcal{C}_{2v} , the finite symmetry group of the scatterer. Then, from the boundary conditions, an infinite set of four linear algebraic equations (each one associated with a given representation) is obtained where the unknown coefficients of the scattered fields are uncoupled. This method significantly simplifies the numerical treatment of the problem. Afterwards, this study has been extended to scatterers of three and four cylinders involving, respectively, the finite symmetry groups \mathcal{C}_{3v} and \mathcal{C}_{4v} [8].

The case of acoustic scattering by two identical spherical bodies (as two spheres or two spherical shells) has been often treated by means of the multiple-scattering method (see references [9–12]) but never by emphasizing all the symmetry properties of the scatterer.

The present work deals with theoretical, numerical and experimental study of the scattering of a plane acoustic wave by two identical spheres. The mathematical formalism developed is based on the techniques of multiple scattering including elements of group theory in order to take into account the symmetries of the two-sphere scatterer. This greatly simplifies the mathematical analysis of the problem. Indeed, when one considers scattering by a sphere, the invariance of the Helmholtz equation under rotations about the centre of the sphere leads to the search of mode solutions by separation of variables of the form $f(r)Y_{lm}(\theta, \phi)$. This is directly linked to the following mathematical results: the spherical harmonics $Y_{lm}(\theta, \phi)$, with l fixed and $m = -l, \dots, +l$, form a basis for the $(2l + 1)$ -dimensional irreducible representation of $O(3)$, the invariance group of the sphere. These mathematical considerations are implicitly used in the partial wave expansions of the incident and scattered fields. In the two-sphere scatterer case, the invariance of a single sphere under the continuous group $O(3)$ is broken, but, however, the full system is invariant under another continuous group, labelled $D_{\infty h}$ in the mathematical literature (see, for example, references [13, 14]).

In section 2, some properties of the continuous group $D_{\infty h}$ are recalled, particularly the symmetry transformations. The incident and scattered fields are expressed as sums of functions belonging to the irreducible representations of $D_{\infty h}$. The unknown coefficients defining the scattered fields are to be determined from the boundary conditions. It should be noted that the use of the symmetry properties allows to uncouple the pairs of unknown coefficients defining the scattered fields. The boundary conditions are then applied at the surface of only one sphere for each irreducible representation. This algebraic approach is valid for general boundary conditions and is displayed in the cases of Neumann boundary conditions (rigid spheres) and elastic boundary conditions (elastic spheres immersed in water). An infinite set of infinite systems of algebraic equations is obtained. Each system, associated with a given representation, can then be solved numerically by truncation and used to obtain the farfield from function. Section 3 deals with numerical and experimental results. The numerical evaluation of the backscattered total form function is carried out in the cases of two rigid spheres and two elastic spheres immersed in water for various geometrical configurations. Moreover, a series of experiments based on ultrasonic spectroscopy is performed in the case of two stainless-steel spheres immersed in water. Experimental data are compared with theoretical ones. The variations of the form function due to the interference phenomenon as well as the sharp minima corresponding to elastic resonances are experimentally observed to be in quite a good agreement with the theory. In section 4, the interest of the method presented in this paper is highlighted and future extensions in the context of multiple scattering suggested.

2. MATHEMATICAL FORMALISM

The scattering of a plane acoustic wave by a system of two identical spheres of radius a is studied. The geometry of the problem as well as the notations used are shown in Figure 1. In particular, the centres of the two spheres are separated by a distance d . Three spherical co-ordinate systems (r, θ, ϕ) , (r_1, θ_1, ϕ) and (r_2, θ_2, ϕ) are defined and, respectively, referred to O , O_1 and O_2 . The propagation vector \mathbf{k} of the incident plane wave is perpendicular to the Oy -axis and forms an angle α with the Oz -axis. In the co-ordinate system (r, θ, ϕ) the incident wave is expressed as

$$\Phi_{inc}(r, \theta, \phi) = \Phi_0 4\pi \sum_{l=0}^{+\infty} \sum_{m=-l}^{+l} i_l^i(kr) Y_{lm}(\theta, \phi) Y_{lm}^*(\alpha, \beta), \quad (1)$$

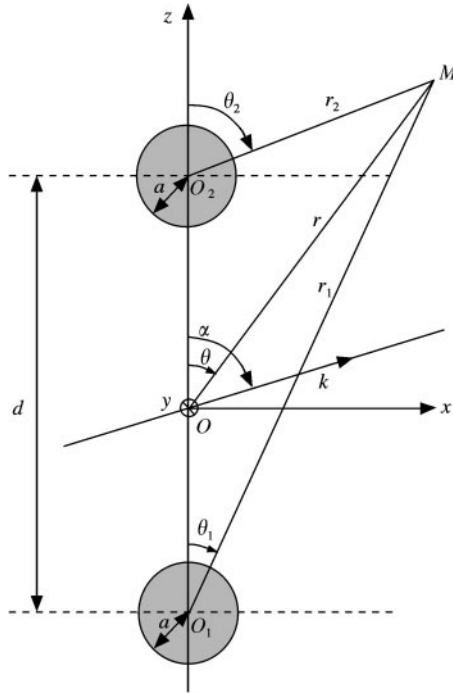


Figure 1. Two-sphere co-ordinate systems.

while the total scattered field from the two spheres can be expressed as

$$\Phi_s = \Phi_s^1(r_1, \theta_1, \phi) + \Phi_s^2(r_2, \theta_2, \phi) \tag{2}$$

with

$$\Phi_s^1(r_1, \theta_1, \phi) = \Phi_0 \sum_{l=0}^{+\infty} \sum_{m=-l}^{+l} A_{lm} h_l^{(1)}(kr_1) Y_{lm}(\theta_1, \phi), \tag{3}$$

$$\Phi_s^2(r_2, \theta_2, \phi) = \Phi_0 \sum_{l=0}^{+\infty} \sum_{m=-l}^{+l} B_{lm} h_l^{(1)}(kr_2) Y_{lm}(\theta_2, \phi). \tag{4}$$

Here and in what follows the $\exp(-i\omega t)$ time dependence is suppressed. j_l and $h_l^{(1)}$, respectively, denote spherical Bessel functions of the first and third kinds, Y_{lm} denotes the spherical harmonics, and A_{lm} and B_{lm} are the unknown scattering coefficients. Usually, this scattering problem is solved by applying boundary conditions for the total field $\Phi_t = \Phi_{inc} + \Phi_s$ at the surface of each sphere. By using addition theorems for spherical wave solutions of the Helmholtz equation [15], an infinite system of two linear complex algebraic equations is then obtained where the unknown coefficients A_{lm} and B_{lm} are coupled.

In order to solve this problem, a new method based on the use of the symmetries of the scatterer is proposed. The two-sphere scatterer, as shown in Figure 1, is invariant under the following symmetry transformations classified in six classes: (1) E the identity transformation; (2) $C(\varphi)$, the rotation through any angle φ about the Oz -axis; (3) σ_v , the mirror reflection in the planes Oyz and Oxz ; (4) I , the inversion; (5) $IC(\varphi)$, the mirror

TABLE 1
Character table of $D_{\infty h}$

$D_{\infty h}$	E	$C(\varphi)$	σ_v	I	$IC(\varphi)$	$I\sigma_v$
$A_{1g} (\Lambda = 0)$	1	1	1	1	1	1
$A_{1u} (\Lambda = 0)$	1	1	1	-1	-1	-1
$A_{2g} (\Lambda = 0)$	1	1	-1	1	1	-1
$A_{2u} (\Lambda = 0)$	1	1	-1	-1	-1	1
$E_{\Lambda g} (\Lambda = 1, 2, \dots + \infty)$	2	$2 \cos (\Lambda\varphi)$	0	2	$2 \cos (\Lambda\varphi)$	0
$E_{\Lambda u} (\Lambda = 1, 2, \dots + \infty)$	2	$2 \cos (\Lambda\varphi)$	0	-2	$-2 \cos (\Lambda\varphi)$	0

reflection in all the planes passing through O and perpendicular to the Oz -axis; (6) $I\sigma_v$, the rotation through π about the Ox - and Oy -axis.

The action of the symmetry transformations on an arbitrary function $\Phi(r, \theta, \phi)$,

$$\Phi(r, \theta, \phi) = \sum_{l=0}^{+\infty} \sum_{m=-l}^{+l} a_{lm} \Phi_l(r) Y_{lm}(\theta, \phi), \tag{5}$$

is given by

$$E\Phi(r, \theta, \phi) = \Phi(r, \theta, \phi), \tag{6}$$

$$C(\varphi)\Phi(r, \theta, \phi) = \Phi(r, \theta, \phi + \varphi), \tag{7}$$

$$\sigma_v\Phi(r, \theta, \phi) = \left\{ \begin{array}{l} \Phi(r, \theta, \pi - \phi) \quad (\text{mirror reflection in the } Oyz \text{ plane}) \\ \Phi(r, \theta, -\phi) \quad (\text{mirror reflection in the } Oxz \text{ plane}) \end{array} \right\}, \tag{8}$$

$$I\Phi(r, \theta, \phi) = \Phi(r, \pi - \theta, \pi + \phi), \tag{9}$$

$$IC(\varphi)\Phi(r, \theta, \phi) = \Phi(r, \pi - \theta, \pi + \phi + \varphi), \tag{10}$$

$$I\sigma_v\Phi(r, \theta, \phi) = \left\{ \begin{array}{l} \Phi(r, \pi - \theta, \phi) \quad (\pi \text{ rotation about the } Ox\text{-axis}) \\ \Phi(r, \pi - \theta, \pi - \phi) \quad (\pi \text{ rotation about the } Oy\text{-axis}) \end{array} \right\}. \tag{11}$$

These transformations form the continuous group of infinite order, labelled $D_{\infty h}$ [13, 14], which constitutes the symmetry group of the scatterer. Four one-dimensional irreducible representations labelled A_{1g} , A_{1u} , A_{2g} , A_{2u} , and an infinite number of two-dimensional irreducible representations labelled E_{1g} , E_{1u} , E_{2g} , E_{2u} , ... $E_{\Lambda g}$, $E_{\Lambda u}$, ... are associated with this symmetry group. They are classified according to $\Lambda = |m|$. For the one-dimensional irreducible representations ($\Lambda = 0$), the group elements E , $C(\varphi)$, σ_v , I , $IC(\varphi)$ and $I\sigma_v$ are represented by 1×1 matrices given in the corresponding column of the character table (Table 1). For the two-dimensional irreducible representations ($\Lambda = 1, 2, \dots, +\infty$), each character of the classes E , $C(\varphi)$, σ_v , I , $IC(\varphi)$ and $I\sigma_v$ is the sum of the diagonal elements, or trace, of the corresponding 2×2 matrices given in Table 2. All the characteristics of $D_{\infty h}$ are gathered in the character table (Table 1). The notations g or u are, respectively, used for irreducible representations which are even or odd under inversion I . Index 1 (respectively 2) is used for the one-dimensional irreducible representations (corresponding to $\Lambda = 0$) which are even (respectively odd) under reflection σ_v . The character table (Table 1) permits one to

TABLE 2

Group elements of the two-dimensional representations of $D_{\infty h}$

	E	$C(\varphi)$	σ_v	I	$IC(\varphi)$	$I\sigma_v$
E_{Ag}	$\begin{pmatrix} 1 & 0 \\ 0 & 1 \end{pmatrix}$	$\begin{pmatrix} e^{iA\varphi} & 0 \\ 0 & e^{-iA\varphi} \end{pmatrix}$	$\begin{pmatrix} 0 & 1 \\ 1 & 0 \end{pmatrix}$	$\begin{pmatrix} 1 & 0 \\ 0 & 1 \end{pmatrix}$	$\begin{pmatrix} e^{iA\varphi} & 0 \\ 0 & e^{-iA\varphi} \end{pmatrix}$	$\begin{pmatrix} 0 & 1 \\ 1 & 0 \end{pmatrix}$
E_{Au}	$\begin{pmatrix} 1 & 0 \\ 0 & 1 \end{pmatrix}$	$\begin{pmatrix} e^{iA\varphi} & 0 \\ 0 & e^{-iA\varphi} \end{pmatrix}$	$\begin{pmatrix} 0 & 1 \\ 1 & 0 \end{pmatrix}$	$\begin{pmatrix} -1 & 0 \\ 0 & -1 \end{pmatrix}$	$\begin{pmatrix} -e^{iA\varphi} & 0 \\ 0 & -e^{-iA\varphi} \end{pmatrix}$	$\begin{pmatrix} 0 & -1 \\ -1 & 0 \end{pmatrix}$

express any function Φ as a sum of functions belonging to the irreducible representations of $D_{\infty h}$

$$\Phi = \Phi^{(\Lambda)} + \sum_{\Lambda=1}^{+\infty} \Phi^{(E_{\Lambda})}, \tag{12}$$

where one defines for the one-dimensional irreducible representations ($\Lambda = |m| = 0$)

$$\Phi^{(\Lambda)} = \Phi^{(A_{1g})} + \Phi^{(A_{1u})} + \Phi^{(A_{2g})} + \Phi^{(A_{2u})}, \tag{13}$$

and for the two-dimensional irreducible representations ($\Lambda = |m| = 1, 2, \dots, +\infty$)

$$\Phi^{(E_{\Lambda})} = \Phi^{(E_{\Lambda g})} + \Phi^{(E_{\Lambda u})}, \tag{14}$$

$$\begin{pmatrix} \Phi^{(E_{m^+})} \\ \Phi^{(E_{m^-})} \end{pmatrix} = \begin{pmatrix} \Phi^{(E_{m^+g})} \\ \Phi^{(E_{m^-g})} \end{pmatrix} + \begin{pmatrix} \Phi^{(E_{m^+u})} \\ \Phi^{(E_{m^-u})} \end{pmatrix}. \tag{15}$$

m^+ and m^- , respectively, stand for the positive and negative values of m ; $m^+ = +1, +2, \dots, +\infty$ and $m^- = -1, -2, \dots, -\infty$.

The incident field defined by equation (1) in the spherical co-ordinate system (r, θ, ϕ) is now written in the spherical co-ordinate system (r_2, θ_2, ϕ) (in which it will be particularly convenient to apply the boundary conditions)

$$\Phi_{inc}(r_2, \theta_2, \phi) = \Phi_0 4\pi e^{i(kd/2)\cos\alpha} \sum_{l=0}^{+\infty} \sum_{m=-l}^{+l} i^l j_l(kr_2) Y_{lm}(\theta_2, \phi) Y_{lm}^*(\alpha, \beta) \tag{16}$$

and modified into the form

$$\begin{aligned} \Phi_{inc}(r_2, \theta_2, \phi) = \Phi_0 4\pi e^{i(kd/2)\cos\alpha} & \left[\sum_{l=0}^{+\infty} i^l j_l(kr_2) Y_{l0}(\theta_2, \phi) Y_{l0}^*(\alpha, \beta) \right. \\ & + \sum_{\Lambda=1}^{+\infty} \sum_{l=\Lambda}^{+\infty} i^l j_l(kr_2) Y_{lm^+}(\theta_2, \phi) Y_{lm^+}^*(\alpha, \beta) \\ & \left. + \sum_{\Lambda=1}^{+\infty} \sum_{l=\Lambda}^{+\infty} i^l j_l(kr_2) Y_{lm^-}(\theta_2, \phi) Y_{lm^-}^*(\alpha, \beta) \right]. \tag{17} \end{aligned}$$

The incident field can now be expressed as a sum of functions belonging to the irreducible representations of $D_{\infty h}$. Using relations (12–15) and (17), one obtains

$$\Phi_{inc}^{(A)} = \Phi_0 4\pi e^{i(kd/2)\cos\alpha} \sum_{l=0}^{+\infty} i^l j_l(kr_2) Y_{l0}(\theta_2, \phi) Y_{l0}^*(\alpha, \beta), \tag{18}$$

$$\Phi_{inc}^{(E_p)} = \Phi_0 4\pi e^{i(kd/2)\cos\alpha} \sum_{l=A}^{+\infty} i^l j_l(kr_2) Y_{lp}(\theta_2, \phi) Y_{lp}^*(\alpha, \beta), \tag{19}$$

where p denotes m^+ or m^- . Furthermore, from the character table of $D_{\infty h}$ (Table 1), the components of the incident field are written as

$$\Phi_{inc}^{(A_{1g})} = K [E + C(\varphi) + \sigma_v \pm I \pm IC(\varphi) \pm I\sigma_v] \Phi_{inc}^{(A)}, \tag{20}$$

$$\Phi_{inc}^{(A_{2g})} = K [E + C(\varphi) - \sigma_v \pm I \pm IC(\varphi) \mp I\sigma_v] \Phi_{inc}^{(A)}, \tag{21}$$

over the one-dimensional representations and

$$\Phi_{inc}^{(E_{pg})} = K' [E + e^{ip\varphi} C(\varphi) \pm I \pm e^{ip\varphi} IC(\varphi)] \Phi_{inc}^{(E_p)}, \tag{22}$$

over the two-dimensional representations. In the previous equations, K and K' are unknown coefficients determined by using relations (13–15), (20–22) and the action of the elements $E, C(\varphi)$ (6, 7) on $\Phi_{inc}^{(A)}, \Phi_{inc}^{(E_p)}$. One obtains

$$K = \frac{1}{8}, \quad K' = \frac{1}{[2(1 + e^{2ip\varphi})]}. \tag{23, 24}$$

So, by using the action (6–11) of the elements of $D_{\infty h}$ and relations (20–24), the incident field is expressed in each irreducible representation as

$$\Phi_{inc}^{(A_{1g})} = \Phi_0 \frac{3\pi}{2} e^{i(kd/2)\cos\alpha} \sum_{l=0}^{+\infty} i^l j_l(kr_2) [1 \pm (-1)^l] Y_{l0}(\theta_2, \phi) Y_{l0}^*(\alpha, \beta), \tag{25}$$

$$\Phi_{inc}^{(A_{2g})} = \Phi_0 \frac{\pi}{2} e^{i(kd/2)\cos\alpha} \sum_{l=0}^{+\infty} i^l j_l(kr_2) [1 \pm (-1)^l] Y_{l0}(\theta_2, \phi) Y_{l0}^*(\alpha, \beta), \tag{26}$$

$$\Phi_{inc}^{(E_{pg})} = \Phi_0 2\pi e^{i(kd/2)\cos\alpha} \sum_{l=A}^{+\infty} i^l j_l(kr_2) [1 \pm (-1)^l] Y_{lp}(\theta_2, \phi) Y_{lp}^*(\alpha, \beta). \tag{27}$$

The total scattered field given in relations (2–4) is

$$\begin{aligned} \Phi_s = \phi_0 & \left\{ \sum_{l=0}^{+\infty} A_{l0} h_l^{(1)}(kr_1) Y_{l0}(\theta_1, \phi) + \sum_{l=0}^{+\infty} B_{l0} h_l^{(1)}(kr_2) Y_{l0}(\theta_2, \phi) \right. \\ & + \sum_{A=1}^{+\infty} \sum_{l=A}^{+\infty} [A_{lm^+} h_l^{(1)}(kr_1) Y_{lm^+}(\theta_1, \phi) + B_{lm^+} h_l^{(1)}(kr_2) Y_{lm^+}(\theta_2, \phi)] \\ & \left. + \sum_{A=1}^{+\infty} \sum_{l=A}^{+\infty} [A_{lm^-} h_l^{(1)}(kr_1) Y_{lm^-}(\theta_1, \phi) + B_{lm^-} h_l^{(1)}(kr_2) Y_{lm^-}(\theta_2, \phi)] \right\}. \tag{28} \end{aligned}$$

Relations (12–15) and (28) lead to

$$\Phi_s^{(A)} = \phi_0 \sum_{l=0}^{+\infty} [h_l^{(1)}(kr_1) A_{l0} Y_{l0}(\theta_1, \phi) + h_l^{(1)}(kr_2) B_{l0} Y_{l0}(\theta_2, \phi)], \quad (29)$$

$$\Phi_s^{(E_p)} = \phi_0 \sum_{l=A}^{+\infty} [h_l^{(1)}(kr_1) A_{lp} Y_{lp}(\theta_1, \phi) + h_l^{(1)}(kr_2) B_{lp} Y_{lp}(\theta_2, \phi)], \quad (30)$$

where p denotes m^+ or m^- . One can now apply the action of the elements of $D_{\infty h}$ on the components $\Phi_s^{(A)}$ and $\Phi_s^{(E_p)}$ of the scattered field. From elementary geometrical considerations and usual relations for the spherical harmonics Y_{lm} [16] this action is defined by

$$E\Phi_s^{(A)} = \phi_0 \sum_{l=0}^{+\infty} [h_l^{(1)}(kr_1) A_{l0} Y_{l0}(\theta_1, \phi) + h_l^{(1)}(kr_2) B_{l0} Y_{l0}(\theta_2, \phi)], \quad (31)$$

$$C(\varphi)\Phi_s^{(A)} = \phi_0 \sum_{l=0}^{+\infty} [h_l^{(1)}(kr_1) A_{l0} Y_{l0}(\theta_1, \phi) + h_l^{(1)}(kr_2) B_{l0} Y_{l0}(\theta_2, \phi)], \quad (32)$$

$$\sigma_v\Phi_s^{(A)} = \phi_0 \sum_{l=0}^{+\infty} [h_l^{(1)}(kr_1) A_{l0} Y_{l0}(\theta_1, \phi) + h_l^{(1)}(kr_2) B_{l0} Y_{l0}(\theta_2, \phi)], \quad (33)$$

$$I\Phi_s^{(A)} = \phi_0 \sum_{l=0}^{+\infty} [h_l^{(1)}(kr_2) A_{l0} Y_{l0}(\theta_2, \phi) + h_l^{(1)}(kr_1) B_{l0} Y_{l0}(\theta_1, \phi)](-1)^l, \quad (34)$$

$$IC(\varphi)\Phi_s^{(A)} = \phi_0 \sum_{l=0}^{+\infty} [h_l^{(1)}(kr_2) A_{l0} Y_{l0}(\theta_2, \phi) + h_l^{(1)}(kr_1) B_{l0} Y_{l0}(\theta_1, \phi)](-1)^l, \quad (35)$$

$$I\sigma_v\Phi_s^{(A)} = \phi_0 \sum_{l=0}^{+\infty} [h_l^{(1)}(kr_2) A_{l0} Y_{l0}(\theta_2, \phi) + h_l^{(1)}(kr_1) B_{l0} Y_{l0}(\theta_1, \phi)](-1)^l \quad (36)$$

for the one-dimensional representations and by

$$E\Phi_s^{(E_p)} = \phi_0 \sum_{l=A}^{+\infty} [A_{lp} h_l^{(1)}(kr_1) Y_{lp}(\theta_1, \phi) + B_{lp} h_l^{(1)}(kr_2) Y_{lp}(\theta_2, \phi)], \quad (37)$$

$$C(\varphi)\Phi_s^{(E_p)} = \phi_0 \sum_{l=A}^{+\infty} [A_{lp} h_l^{(1)}(kr_1) Y_{lp}(\theta_1, \phi) + B_{lp} h_l^{(1)}(kr_2) Y_{lp}(\theta_2, \phi)] e^{ip\varphi}, \quad (38)$$

$$I\Phi_s^{(E_p)} = \phi_0 \sum_{l=A}^{+\infty} [B_{lp} h_l^{(1)}(kr_1) Y_{lp}(\theta_1, \phi) + A_{lp} h_l^{(1)}(kr_2) Y_{lp}(\theta_2, \phi)](-1)^l, \quad (39)$$

$$IC(\varphi)\Phi_s^{(E_p)} = \phi_0 \sum_{l=A}^{+\infty} [B_{lp} h_l^{(1)}(kr_1) Y_{lp}(\theta_1, \phi) + A_{lp} h_l^{(1)}(kr_2) Y_{lp}(\theta_2, \phi)](-1)^l e^{ip\varphi} \quad (40)$$

for the two-dimensional representations. The total scattered field is defined as

$$\Phi_s^{(A_{10}^p)} = \phi_0 \sum_{l=0}^{+\infty} [h_l^{(1)}(kr_1) A_{l0}^{(A_{10}^p)} Y_{l0}(\theta_1, \phi) + h_l^{(1)}(kr_2) B_{l0}^{(A_{10}^p)} Y_{l0}(\theta_2, \phi)], \quad (41)$$

$$\Phi_s^{(A_{2g})} = \phi_0 \sum_{l=0}^{+\infty} [h_l^{(1)}(kr_1) A_{l0}^{(A_{2g})} Y_{l0}(\theta_1, \phi) + h_l^{(1)}(kr_2) B_{l0}^{(A_{2g})} Y_{l0}(\theta_2, \phi)], \tag{42}$$

$$\Phi_s^{(E_{pg})} = \phi_0 \sum_{l=A}^{+\infty} [h_l^{(1)}(kr_1) A_{lp}^{(E_{pg})} Y_{lp}(\theta_1, \phi) + h_l^{(1)}(kr_2) B_{lp}^{(E_{pg})} Y_{lp}(\theta_2, \phi)], \tag{43}$$

where A_{lp} and B_{lp} are the unknown scattering coefficients written for each irreducible representation of $D_{\infty h}$. Moreover, the character table of $D_{\infty h}$ (Table 1) gives

$$\Phi_s^{(A_{1g})} = K [E + C(\varphi) + \sigma_v \pm I \pm IC(\varphi) \pm I\sigma_v] \Phi_s^{(A)}, \tag{44}$$

$$\Phi_s^{(A_{2g})} = K [E + C(\varphi) - \sigma_v \pm I \pm IC(\varphi) \mp I\sigma_v] \Phi_s^{(A)}, \tag{45}$$

$$\Phi_s^{(E_{pg})} = K' [E + e^{ip\varphi} C(\varphi) \pm I \pm e^{ip\varphi} IC(\varphi)] \Phi_s^{(E_p)}. \tag{46}$$

where K and K' are the coefficients previously determined in equations (23, 24). Using equations (31–40), (41–43) and (44–46), one finds that the scattering coefficients must satisfy

$$B_{l0}^{(A_{1g})} = \pm (-1)^l A_{l0}^{(A_{1g})}, \tag{47}$$

$$B_{l0}^{(A_{2g})} = \pm (-1)^l A_{l0}^{(A_{2g})}, \tag{48}$$

$$B_{lp}^{(E_{pg})} = \pm (-1)^l A_{lp}^{(E_{pg})}. \tag{49}$$

It appears from relations (47–49) that the coefficients defining the scattered field are uncoupled; only one series of coefficients is associated with a given irreducible representation. Finally, from equations (41–43) and (47–49), the decomposition of the total scattered field over the irreducible representations of $D_{\infty h}$ is given by

$$\Phi_s^{(A_{1g})} = \phi_0 \sum_{l=0}^{+\infty} A_{l0}^{(A_{1g})} [h_l^{(1)}(kr_1) Y_{l0}(\theta_1, \phi) \pm (-1)^l h_l^{(1)}(kr_2) Y_{l0}(\theta_2, \phi)], \tag{50}$$

$$\Phi_s^{(A_{2g})} = \phi_0 \sum_{l=0}^{+\infty} A_{l0}^{(A_{2g})} [h_l^{(1)}(kr_1) Y_{l0}(\theta_1, \phi) \pm (-1)^l h_l^{(1)}(kr_2) Y_{l0}(\theta_2, \phi)], \tag{51}$$

$$\Phi_s^{(E_{pg})} = \phi_0 \sum_{l=A}^{+\infty} A_{lp}^{(E_{pg})} [h_l^{(1)}(kr_1) Y_{lp}(\theta_1, \phi) \pm (-1)^l h_l^{(1)}(kr_2) Y_{lp}(\theta_2, \phi)]. \tag{52}$$

Generally, the unknown scattering coefficients are determined from the boundary conditions at the surface of the spheres. In fact, because account has been taken of the symmetries of the scatterer, one just has to apply boundary conditions at the surface of only one sphere. Besides, boundary conditions are separately written in each irreducible representation. For example, in the case of Dirichlet boundary conditions (soft spheres), one can write

$$(\Phi_{inc}^{(X)} + \Phi_s^{(X)})_{r_2=a} = 0, \tag{53}$$

where X denotes A_{1g} , A_{1u} , A_{2g} , A_{2u} , E_{pg} or E_{pu} . The addition theorem [15]

$$h_l^{(1)}(kr_1) Y_{lm}(\theta_1, \phi) = \sum_{l'=0}^{+\infty} \sum_{\lambda=0}^{+\infty} C(lm|l'0|\lambda m) j_\lambda(kr_2) Y_{\lambda m}(\theta_2, \phi) h_l^{(1)}(kd) \sqrt{\frac{2l'+1}{4\pi}} \tag{54}$$

allows one to express the scattered field (50–52) in the co-ordinate system (r_2, θ_2, ϕ) . The $C(lm|l'm'|\lambda\mu)$ coefficients are defined from Wigner symbols by

$$C(lm|l'm'|\lambda\mu) = i^{-l+l'+\lambda}(-1)^m \sqrt{4\pi(2l+1)(2l'+1)(2\lambda+1)} \\ \times \begin{pmatrix} l & l' & \lambda \\ 0 & 0 & 0 \end{pmatrix} \begin{pmatrix} l & l' & \lambda \\ -m & m' & \mu \end{pmatrix}. \tag{55}$$

Finally, equation (53) leads to

$$\sum_{\lambda=0}^{+\infty} (\delta_{l\lambda} \mp M_{l\lambda}^{(0)}) A_{\lambda 0}^{(A_{1p})} = \alpha_l^{(A_{1p})} S_l(ka), \tag{56}$$

$$\sum_{\lambda=0}^{+\infty} (\delta_{l\lambda} \mp M_{l\lambda}^{(0)}) A_{\lambda 0}^{(A_{2p})} = \alpha_l^{(A_{2p})} S_l(ka), \tag{57}$$

$$\sum_{\lambda=0}^{+\infty} (\delta_{l\lambda} \mp M_{l\lambda}^{(p)}) A_{\lambda p}^{(E_{rp})} = \alpha_l^{(E_{rp})} S_l(ka), \tag{58}$$

where the matrices $M_{l\lambda}^{(0)}$ and $M_{l\lambda}^{(p)}$ are given by

$$M_{l\lambda}^{(0)} = \sum_{l'=0}^{+\infty} (-1)^l C(\lambda 0 | l 0 | l' 0) S_l(ka) h_{l'}^{(1)}(kd) \sqrt{\frac{2l'+1}{4\pi}}, \tag{59}$$

$$M_{l\lambda}^{(p)} = \sum_{l'=0}^{+\infty} (-1)^l C(\lambda p | l p | l' 0) S_l(ka) h_{l'}^{(1)}(kd) \sqrt{\frac{2l'+1}{4\pi}}. \tag{60}$$

The vector $S_l(ka)$ which includes Dirichlet boundary conditions is given by

$$S_l(ka) = -\frac{j_l(ka)}{h_l^{(1)}(ka)}, \tag{61}$$

while the vectors defining the incident wave are written as

$$\alpha_l^{(A_{1p})} = \frac{3\pi}{2} e^{i(kd/2)\cos\alpha} i^l [1 \pm (-1)^l] Y_{l0}^*(\alpha, \beta), \tag{62}$$

$$\alpha_l^{(A_{2p})} = \frac{\pi}{2} e^{i(kd/2)\cos\alpha} i^l [1 \pm (-1)^l] Y_{l0}^*(\alpha, \beta), \tag{63}$$

$$\alpha_l^{(E_{rp})} = 2\pi e^{i(kd/2)\cos\alpha} i^l [1 \pm (-1)^l] Y_{lp}^*(\alpha, \beta). \tag{64}$$

Our algebraic approach developed for soft spheres is also valid for more general boundary conditions. The scattering problem remains governed by equations (56–60) and equations (62–64). It is only necessary to modify the vector $S_l(ka)$ in order to take into account particular boundary conditions. In case of the Neumann boundary conditions (rigid spheres), the vanishing of the normal derivative of the total field yields

$$S_l(ka) = -\frac{j'_l(ka)}{h_l^{(1)'}(ka)}. \tag{65}$$

For two elastic spheres immersed in water, one obtains

$$S_l(ka) = - \frac{D_l^{[1]}(ka)}{D_l^{[2]}(ka)} \tag{66}$$

from the continuity of normal displacements and stress continuity relations. Here $D_l^{[1]}$ and $D_l^{[2]}$ are the usual determinants of third rank with coefficients depending on the longitudinal and transverse velocities in the solid and the sound velocity in the liquid [17].

Therefore, the scattering of a plane acoustic wave by a system of two identical spheres reduces to the solution of equations (56–58), an infinite set of infinite systems of linear complex algebraic equations. Each system is associated with a given irreducible representation of $D_{\infty h}$. The unknown scattering coefficients are uncoupled due to the symmetry considerations, this greatly simplifies the treatment of the problem. The systems of equations can then be numerically solved by truncation and used to obtain the farfield form function [18] of the system for various angles of incidence α , angles of scattering θ and separation distances d .

The form function FF_∞ in the direction (θ, ϕ) is defined by

$$FF_\infty(\theta, \phi) = \lim_{r \rightarrow \infty} \frac{2r}{a} \left| \frac{\Phi_s}{\Phi_{inc}} \right|. \tag{67}$$

By taking the limit of each component of the scattered field, one obtains

$$FF_\infty(\theta, \phi) = \frac{2}{ka} |f^{(A_{1g})} + f^{(A_{1u})} + f^{(A_{2g})} + f^{(A_{2u})} + \sum_{A=1}^{+\infty} [f^{(E_{pg})} + f^{(E_{pu})}]|, \tag{68}$$

where

$$f^{(A_{1g})} = \sum_{l=0}^{+\infty} A_{l0}^{(A_{1g})} Y_{l0}(\theta, \phi) e^{-il\pi/2} [e^{i(kd/2)\cos\theta} \pm (-1)^l e^{-i(kd/2)\cos\theta}], \tag{69}$$

$$f^{(A_{2g})} = \sum_{l=0}^{+\infty} A_{l0}^{(A_{2g})} Y_{l0}(\theta, \phi) e^{-il\pi/2} [e^{i(kd/2)\cos\theta} \pm (-1)^l e^{-i(kd/2)\cos\theta}], \tag{70}$$

$$f^{(E_{pg})} = \sum_{l=A}^{+\infty} A_{lp}^{(E_{pg})} Y_{lp}(\theta, \phi) e^{-il\pi/2} [e^{i(kd/2)\cos\theta} \pm (-1)^l e^{-i(kd/2)\cos\theta}], \tag{71}$$

From now on, interest is focused on the study of the form function for various geometrical configurations and boundary conditions.

3. NUMERICAL RESULTS AND COMPARISON WITH EXPERIMENT

3.1. NUMERICAL CONSIDERATIONS

The determination of the total form function depends on the evaluation of the unknown scattering coefficients. These coefficients are found by solving the truncated complex linear systems, equations (56–58), exactly. The infinite matrices $M_{l\lambda}^{(0)}$ and $M_{l\lambda}^{(p)}$ are, respectively,

replaced by associated matrices of rank $(N + 1)$ and $(N + 1 - A)$, with

$$N = \text{sup}(8, [ka + 4(ka)^{1/3} + 1]). \quad (72)$$

The above truncation order N has been chosen from the numerical discussions of Young and Bertrand [2] and Nussenzweig [19], and it has been numerically tested. This truncation order ensure a seven-digit accuracy in the computations. The unknown coefficients are determined for each irreducible representation, and numerical results of the total form function are then obtained from equation (68). The matrices involved in the calculations are well conditioned and they are directly solved by using the standard Gaussian elimination method. The main advantage is to obtain uncoupled equations that can be solved separately for each irreducible representation. It should be noted that another method to solve this scattering problem has been already published [9–11]. In order to give a rough idea of how much our method is better adapted to numerical calculations a simple comparison is presented below.

Method of Gaunard et al. ([9–11])

Two systems of $(N + 1 - p)$ coupled equations must be solved, with $p = 0, 1, \dots, N$ and N chosen to ensure five-digit accuracy. As noted by the authors, the matrices involved in the calculations are severely ill conditioned and they do not admit solution by direct method (standard Gaussian elimination). An iterative method (Gauss–Seidel) is used requiring no more than 15 iterations to ensure the convergence at the desired five-digit accuracy for low p values. Furthermore, in the context of acoustic scattering by two elastic spherical shells [11], the Gauss–Seidel method diverges in the neighborhoods of resonance frequencies when the shells are close to other. Finally, the $C(lm|l'm'|\lambda\mu)$ coefficients are obtained by using a recurrence relation.

Our method

Four systems of $(N + 1 - p)$ uncoupled equations must be solved, with $p = 0, 1, \dots, N$ and N chosen to ensure seven digits accuracy. The matrices involved in the calculations are well conditioned and they are directly solved using standard Gaussian elimination method. Furthermore, we have tested our method in the context of acoustic scattering by two elastic spherical shells. Even in the configuration leading to computational difficulties in reference [11] (shells close to each other), the matrices remain well conditioned and the results are still obtained by the standard Gaussian elimination method. The explicit expressions of the $C(lm|l'm'|\lambda\mu)$ coefficients (55) have been beforehand performed for the maximal value $N_{max} = 40$ by using a software application performing exact calculus (Mathematica [20]), these coefficients are then truncated at the double precision machine size format (15 digits accuracy) and stored.

Then, the numerical evaluation of the backscattered ($\theta = \alpha + \pi$) total form function has been carried out in cases of the two rigid spheres (Neumann boundary conditions) and the two elastic spheres (elastic boundary conditions) for various angles of incidence α and separation distances d .

3.2. RIGID SPHERES

The results of the farfield form function for two rigid spheres, versus the non-dimensional wavenumber ka (in the restricted domain $0 \leq ka \leq 27$), are displayed in Figures 2–4 for separation distances of $d = 2a$ and $4a$. Figure 2, Figure 3 and Figure 4, respectively, display the cases of end-on incidence ($\alpha = 0$), broadside incidence ($\alpha = \pi/2$) and oblique incidence

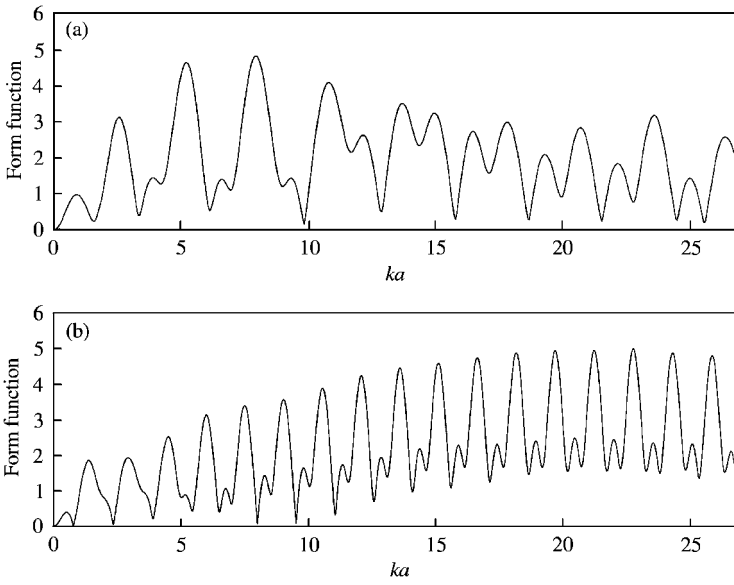


Figure 2. Computed form functions of two rigid spheres at end-on incidence ($\alpha = 0$) versus ka for the separation distances: (a) $d = 2a$, (b) $d = 4a$.

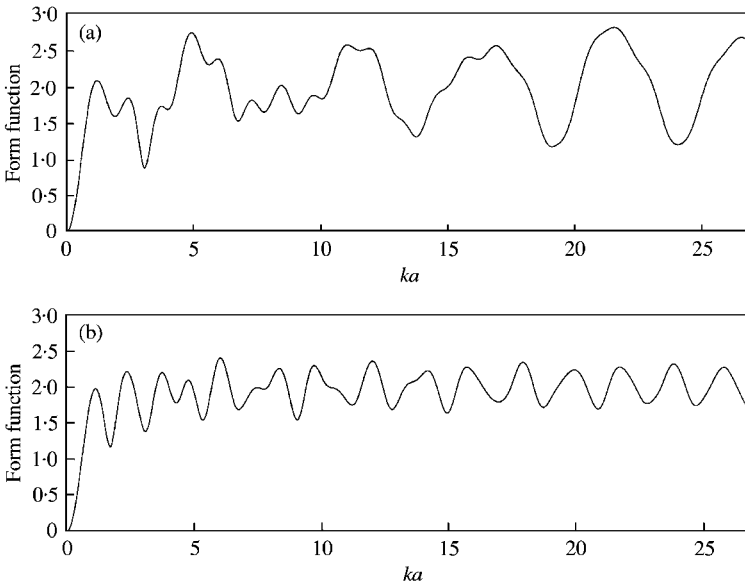


Figure 3. Computed form functions of two rigid spheres at broadside incidence ($\alpha = \pi/2$) versus ka for the separation distances: (a) $d = 2a$, (b) $d = 4a$.

($\alpha = \pi/4$). The variations of the total form function only depend on the interference phenomenon due to the scattered waves by the two spheres. The oscillations are more important as the separation distance grows. The computed results match those presented in the study of Gaunard *et al.* [10] for the backscattering form function of two rigid spheres. The study of these variations is not the main purpose of this present work, further details are

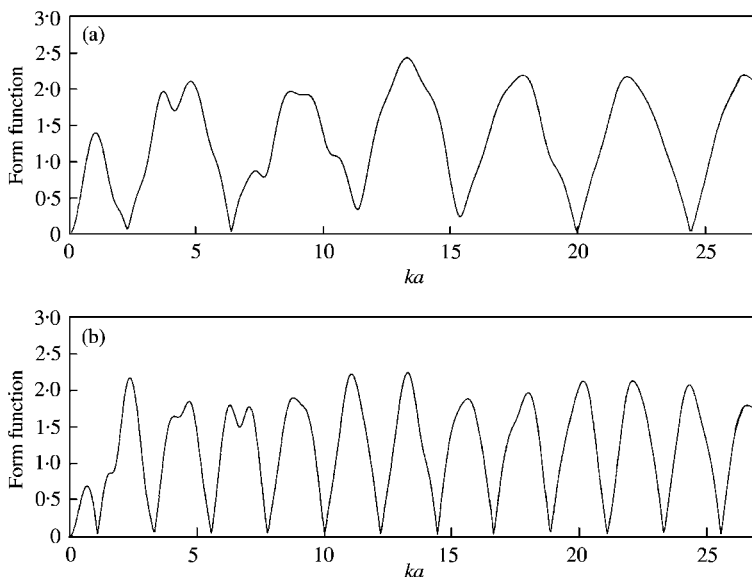


Figure 4. Computed form functions of two rigid spheres at oblique incidence ($\alpha = \pi/4$) versus ka for the separation distances: (a) $d = 2a$, (b) $d = 4a$.

available in reference [10]. It should be noted that symmetry considerations permits one to uncouple the scattering coefficients. Moreover, the matrices involved in calculations are better conditioned than those corresponding to the associated coupled problem; therefore, this method greatly simplifies the numerical treatment of the problem and speeds up calculations.

3.3. ELASTIC SPHERES IMMERSED IN WATER

Numerical calculations and a series of experiments have been performed in the case of scattering of acoustic waves from two stainless-steel spheres immersed in water. The computations are carried out for the following parameters: water ($\rho_0 = 1 \text{ g/cm}^3$, $c = 1480 \text{ m/s}$) and stainless-steel (AFN Z30C13) spheres ($\rho = 7.6911 \text{ g/cm}^3$, $c_t = 6062.7 \text{ m/s}$, $c_l = 3240.6 \text{ m/s}$).

3.3.1. Experimental set-up

The experimental results are obtained by ultrasonic spectroscopy. This method consists of using short ultrasonic pulses for excitation and calculating the Fourier transform by a fast Fourier transform (FFT) algorithm of the gated-averaged signal reflected from the two spheres of radius $a = 1.5 \text{ cm}$. The experiment has been carried out in a monostatic configuration; only one ultrasonic transducer is used both for emission and reception (backscattering). The usable frequency bandwidth ranges from 250 to 700 kHz which corresponds to the restricted ka domain $16 \leq ka \leq 44.5$. The received signal is amplified, averaged, sampled and stored in order to perform further calculations by FFT. The intensity spectra calculated are then normalized by those obtained from a perfectly reflecting surface. This permits one to eliminate the frequency response of the transducer

and the perturbations produced by the electronic measure chain. In this way, one can directly compare the theoretical and experimental results.

3.3.2. Comparison between numerical and experimental results

Experimental data are compared with the theoretical form function calculated from equation (68) in Figures 5–7. The smooth variations of the total form function with ka are due to the interferences between the waves scattered by the spheres as in case of the two rigid spheres. Furthermore, numerous rapid variations of sharp characteristic shape, which are theoretically predicted, can be experimentally observed. They correspond to elastic resonances linked to the eigenfrequencies of the elastic vibrations of the scatterer.

Figures 5 and 6 display the comparison between the theoretical and experimental results in case of the broadside incidence ($\alpha = \pi/2, \theta = 3\pi/2$) for the separation distances $d = 2a$ and $4a$. Experimental results show reasonable agreement with those obtained by computation particularly in the interval $16 \leq ka \leq 27$ which is included in the frequency bandwidth of the transducer. The upper limit of ka in the calculations is due to the maximal value $N_{max} = 40$ used in the evaluation of the $C(lm|l'm'|\lambda\mu)$ coefficients. In the domain $ka < 16$, small perturbations appear in the signal because of the limited bandwidth of the transducer used. The variations of the form function due to the interference phenomenon as well as the sharp minima corresponding to elastic resonances are experimentally observed to be in quite a good agreement with the theory. When the two spheres are touching each other ($d = 2a$), a relative discrepancy between the theoretical and experimental results is observed (Figure 5). This can be interpreted by the waves scattered from the fixing points of the spheres.

In case of the end-on incidence ($\alpha = 0, \theta = \pi$) for a separation distance $d = 2a$ (Figure 7), the experimental results do not agree with the theoretical ones. The interference phenomenon is then strongly dependent on the angular precision of the transducer

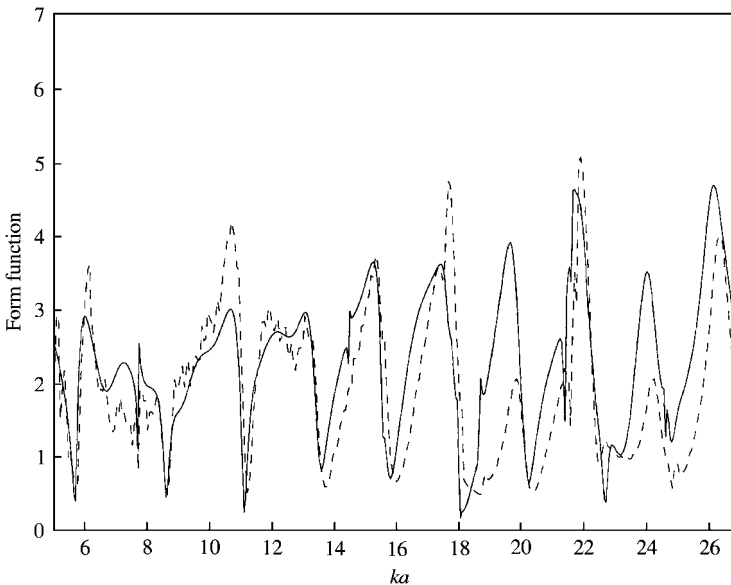


Figure 5. Form functions of two stainless-steel spheres immersed in water at broadside incidence ($\alpha = \pi/2$) versus ka for the separation distance $d = 2a$: —, theory; --, experiment.

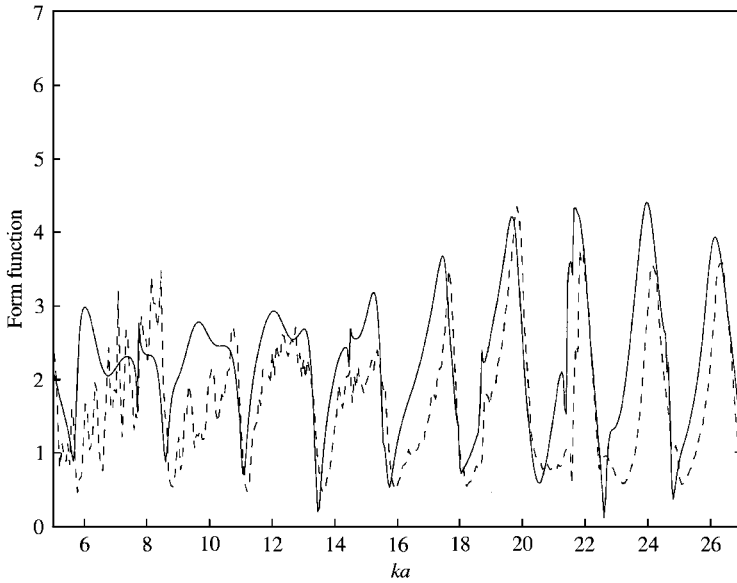


Figure 6. Form functions of two stainless-steel spheres immersed in water at broadside incidence ($\alpha = \pi/2$) versus ka for the separation distance $d = 4a$: —, theory; --, experiment.

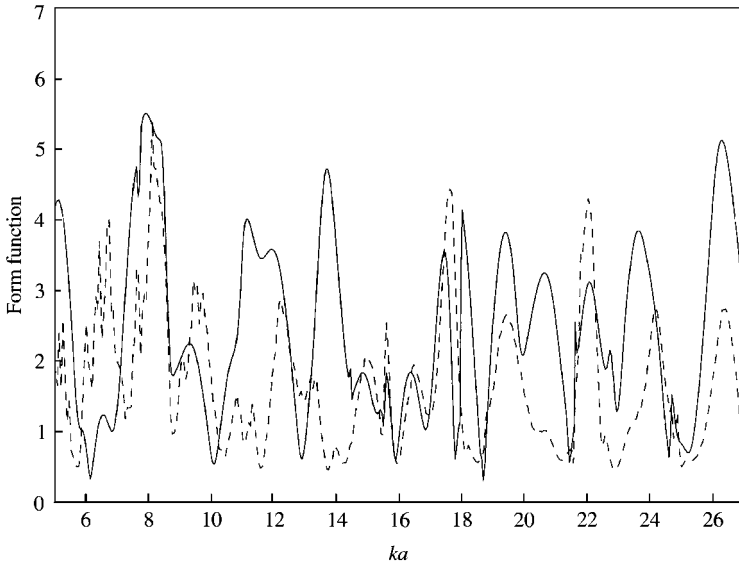


Figure 7. Form functions of two stainless-steel spheres immersed in water at end-on incidence ($\alpha = 0$) versus ka for the separation distance $d = 2a$: —, theory; --, experiment.

positioning. Moreover, such a configuration, which requires a perfect alignment of the two-sphere system with the transducer, is very difficult to obtain.

4. CONCLUSIONS AND PERSPECTIVES

In this paper, an exact formalism has been developed in order to calculate the total scattered field by two identical spheres. This new approach, applied for the first time in this

context, includes symmetry considerations of the scatterer system. The use of group representation theory permits one to obtain, for each irreducible representation of $D_{\infty h}$ (the symmetry group of the scatterer), an infinite system of algebraic equations where the unknown scattering coefficients are uncoupled. This feature greatly simplifies the treatment of the problem and speeds up calculations. Numerical computations have been carried out in the cases of Neumann boundary conditions (rigid spheres) and elastic boundary conditions (elastic spheres immersed in water). It should be noted that the formalism developed here can be easily extended to other realistic physical problems by taking into account various boundary conditions.

Furthermore, a series of experiments based on ultrasonic spectroscopy has been performed in the case of two stainless-steel spheres immersed in water. The experimental form functions are compared with the theoretical ones. The variations due to the interference phenomenon as well as the sharp minima corresponding to elastic resonances are experimentally observed in quite a good agreement with the theory in case of the broadside incidence.

This new approach can also be applied to other multiple scattering problems such as sound scattering from two non-identical spheres (the symmetry group involved is $\mathcal{C}_{\infty v}$), two spherical shells, or an arbitrary number of spherical objects when symmetries are present (for instance, three spheres centred at the vertices of an equilateral triangle and involving the D_{3h} symmetry group).

Moreover, it would be interesting to search the location of the resonances in the complex ka -plane following the method developed in reference [7] for two-dimensional problems. This would allow one to classify the resonances according to the $(2l + 4)$ irreducible representations of $D_{\infty h}$. Therefore, one could also observe the splitting up the elastic resonances (associated with only one sphere) due to the symmetry breaking in the transition from the symmetry group $O(3)$ to $D_{\infty h}$. It would be interesting to experimentally confirm these physical effects.

ACKNOWLEDGMENT

The authors would like to thank Antoine Folacci for useful discussions.

REFERENCES

1. J. E. BURKE and V. TWERSKY 1964 *Journal Research National Bureau Standards* **88D**, 500–510. On scattering of waves by many bodies.
2. J. W. YOUNG and J. C. BERTRAND 1975 *Journal of the Acoustical Society of America* **58**, 1190–1195. Multiple scattering by two cylinders.
3. L. D. LANDAU and E. M. LIFSHITZ 1975 *Quantum Mechanics*. Oxford: Pergamon.
4. A. KUDROLLI and S. SRIDHAR 1997 in *Microwave 2-disk Scattering* MA, Cambridge: (D. H. Feng and B. L. Hu, editors) International Press. Quantum-classical correspondence.
5. P. GASPARD and S. A. RICE 1989 *Journal of Chemical Physics* **90**, 2255–2262. Exact quantization of the scattering from a classically chaotic repeller.
6. P. CVITANOVIĆ and B. ECKHARDT 1993 *Nonlinearity* **6**, 277–311. Symmetry decomposition of chaotic dynamics.
7. Y. DECANINI, A. FOLACCI, P. GABRIELLI and J. L. ROSSI 1998 *Journal of Sound and Vibration* **221**, 785–804. Algebraic aspects of multiple scattering by two parallel cylinders: classification and physical interpretation of scattering resonances.
8. Y. DECANINI, A. FOLACCI, E. FOURNIER and P. GABRIELLI 1998 *Journal of Physics A: Mathematical and General* **31**, 7865–7900. Exact S -matrix for N -disc systems and various boundary conditions: I. Generalization of the Korringa–Kohn–Rostoker–Berry method, II. Determination and partial classification of resonances.

9. G. C. GAUNAURD and H. HUANG 1994 *Journal of the Acoustical Society of America* **96**, 2526–2536. Acoustic scattering by a spherical body near a plane boundary.
10. G. C. GAUNAURD, H. HUANG and H. C. STRIFORS 1995 *Journal of the Acoustical Society of America* **98**, 495–507. Acoustic scattering by a pair of spheres.
11. H. HUANG and G. C. GAUNAURD 1995 *Journal of the Acoustical Society of America* **98**, 2149–2156. Acoustic scattering of a plane wave by two spherical elastic shells.
12. J. L. ROSSI 1996 *Thèse de doctorat de l'université de Corse*. Diffusion acoustique par deux cibles élastiques de forme géométrique sphérique.
13. V. HEINE 1960 *Group Theory in Quantum Mechanics*. New York: Dover.
14. M. HAMERMESH 1962 *Group Theory and its Application to Physical Problems*. New York: Dover.
15. B. U. FELDERHOF and R. B. JONES 1987 *Journal of Mathematical Physics* **28**, 836–839. Addition theorems for spherical wave solutions of the vector Helmholtz equation.
16. G. ARKFEN 1985 *Mathematical Methods for Physicists*. London: Academic Press.
17. G. C. GAUNAURD and H. ÜBERALL 1983 *Journal of the Acoustical Society of America* **73**, 1–12. RST analysis of monostatic and bistatic acoustic echoes from an elastic sphere.
18. N. D. VEKSLER 1993 *Resonance Acoustic Spectroscopy*. Berlin: Springer-Verlag.
19. H. M. NUSSENZVEIG 1992 *Diffraction Effects in Semiclassical Scattering*. Cambridge: Cambridge University Press.
20. S. WOLFRAM 1999 *The Mathematica Book*. Wolfram Media: Cambridge University Press; fourth edition.